Science and Technology Indonesia
e-ISSN:2580-4391 *p*-ISSN:2580-4405
Vol. 11, No. 1, January 2026

Research Paper

Formulation Optimization and In Vitro Antioxidant Evaluation of a Polyherbal Nanosuspension Incorporating *Apium graveolens, Centella asiatica*, and *Orthosiphon stamineus*

Febriana Astuti[1,3], Akrom[1*], Mustofa[2], Arif Budi Setianto[1], Titiek Hidayati[4]

[1]*Doctoral Research Program of Pharmacy Sciences, Faculty of Pharmacy, Universitas Ahmad Dahlan, Yogyakarta, 55191, Indonesia*
[2]*Faculty of Medicine, Public Health and Nursing, Gadjah Mada University, Yogyakarta, 55281, Indonesia*
[3]*D3 Pharmacy Research Program, Politeknik Kesehatan TNI AU Adisutjipto, Yogyakarta, 55198, Indonesia*
[4]*Medical Study Programme, University of Muhammadiyah Yogyakarta, Yogyakarta, 55181, Indonesia*
***Corresponding author**: akrom@pharm.uad.ac.id*

Abstract
Antioxidants play a crucial role in protecting cells from damage caused by free radicals, particularly reactive oxygen species (ROS). Herbal plants contain various bioactive compounds, such as phenolics, flavonoids, terpenoids, and alkaloids, which exhibit strong antioxidant properties to neutralize these harmful molecules. However, the bioavailability of these compounds is often limited due to their poor water solubility. Nanotechnology offers a promising solution, specifically through the development of nanosuspensions. This approach enhances the solubility of these compounds by reducing their particle size to the nanometer scale, thus improving absorption in the body. In this study, nanosuspensions were formulated using extracts from *Apium graveolens*, *Centella asiatica*, and *Orthosiphon stamineus* through a two-factor optimization approach with Design-Expert® version 13 software. The optimal formulation contained $25\,\mathrm{mL}$ of chitosan, $6\,\mathrm{g}$ of Tween 80, and $10\,\mathrm{mL}$ of sodium tripolyphosphate (Na-TPP), resulting in nanosuspensions with an average particle size of $220.00(1157)\,\mathrm{nm}$, a polydispersity index (PDI) of 0.59 ± 0.06, and a zeta potential of -28.27 ± 0.37 mV. The antioxidant activity was evaluated using DPPH and ABTS assays. In the DPPH assay, the nanopolyherbal formulation showed an IC_{50} of $41.780(3064)\,\mu\mathrm{g\,mL^{-1}}$, while the combined extract had an IC_{50} of $44.930(2989)\,\mu\mathrm{g\,mL^{-1}}$. The ABTS assay revealed an IC_{50} of $28.21\,\mu\mathrm{g\,mL^{-1}}$ for the nanosuspension, significantly lower than the combined extract's $54.22\,\mu\mathrm{g\,mL^{-1}}$. These results highlight the superior antioxidant activity of the nanosuspension, emphasizing the potential of nanotechnology to enhance the efficacy of bioactive compounds from herbal plants.

Keywords
Optimization, Nanosuspensions, Antioxidant, Extract Herbals

Received: 8 June 2025, Accepted: 18 September 2025
https://doi.org/10.26554/sti.2026.11.1.65-83

1. INTRODUCTION

The use of herbal medicines as alternative treatments has grown in popularity, reflecting a broader appreciation for natural remedies that are generally safer and cause fewer side effects compared to synthetic drugs (Hassanpour and Doroudi, 2023; Wang et al., 2023). Herbal plants like *Apium graveolens, Centella asiatica,* and *Orthosiphon stamineus* are known for their beneficial chemical makeup, which includes substances that can fight oxidation, reduce inflammation, and kill germs, making them useful for various health problems (Mohamud Dirie et al., 2025; Muchtaridi et al., 2023; Wei et al., 2025). The antioxidant effects of these compounds play a crucial role in reducing cellular damage caused by free radicals, which contribute to the development of degenerative conditions such as cancer, diabetes, and cardiovascular diseases (Abbasnezhad et al., 2022; Hafiz et al., 2020; Ho et al., 2014). Consequently, these medicinal plants may serve as valuable sources of antioxidants with significant health benefits, underscoring the importance of developing improved herbal formulations.

A major challenge in developing herbal medicines is the poor water solubility of active compounds, which often hinders their absorption in the body and reduces therapeutic effectiveness (Awlqadr et al., 2025). Because of this low solubility, only a limited portion of these compounds is absorbed, restricting their potential health benefits (Liu et al., 2024). Nanotechnology, particularly the use of nanosuspensions, presents a promising solution to overcome this limitation (Huang et al., 2024; Zhuo et al., 2024). Nanosuspensions consist of very

small drug particles-less than one micrometer in size-dispersed within a liquid medium. This dispersion enhances the dissolution of the active compounds by expanding the surface area of the particles (Patel and Agrawal, 2011). This approach also facilitates better absorption of active compounds through different biological barriers, including the skin and gastrointestinal tract, which in turn increases bioavailability and improves the overall effectiveness of herbal medicines (Pınar et al., 2023).

Nanosuspensions are biphasic systems where pure drug particles are dispersed in an aqueous medium and stabilized by surfactants (Singh et al., 2018). They provide several advantages, including enhanced solubility, reduced variability associated with food intake during oral administration, better adhesion to surfaces and cell membranes, increased bioavailability, as well as easier formulation and scalability (Kheradkar and M., 2023). Nanosuspensions are characterized by a narrow particle size distribution and precise drug content, making them well-suited for a wide range of medications, particularly those with poor water or liquid solubility. Additionally, they do not cause blockages in blood capillaries (Jacob et al., 2025; Patel and Agrawal, 2011). Nanosuspension drug delivery systems can be administered as liquid formulations or converted into solid forms such as powders, tablets, pellets, capsules, or films. These nanosuspensions are versatile and can be safely delivered through various routes, including oral, intravenous, ophthalmic, topical, and pulmonary administration (Jacob et al., 2025).

Previous studies have mainly focused on single plant extracts like *Apium graveolens, Centella asiatica,* and *Orthosiphon stamineus* to evaluate their antioxidant, anti-inflammatory, and antibacterial effects (Han Jie et al., 2021; Kazi et al., 2020; Kandasamy et al., 2023). Although individual plant extracts have demonstrated significant therapeutic potential, their effectiveness is often hindered by issues such as poor solubility and low bioavailability. This study introduces a novel nanosuspension combining extracts from *Apium graveolens, Centella asiatica,* and *Orthosiphon stamineus* a formulation not previously explored. The formulation enhances the medicinal properties of each plant by improving solubility and bioavailability of their active compounds. Moreover, this study systematically optimizes the formulation to achieve the best particle size, polydispersity index, stability, ensuring a stable and consistent product. The goal of this combination is to enhance the medicinal properties of each plant by improving the solubility and bioavailability of their active compounds. By reducing particle size to below one micrometer, the nanosuspension increases surface area, thereby facilitating better absorption and improving the overall efficacy of the treatment. This innovative formulation addresses the limitations commonly associated with poorly soluble herbal extracts, strengthens the synergistic effects of the combined herbs, and enhances their antioxidant and therapeutic activities (Chavhan, 2025; Chavda et al., 2025).

This study seeks to develop a nanosuspension composed of extracts from *Apium graveolens, Centella asiatica,* and *Orthosiphon stamineus* using a novel approach not previously investigated. The optimized formulation will be evaluated based on particle size, polydispersity index, and stability parameters. Additionally, the antioxidant potential of the nanosuspension will be assessed through DPPH and ABTS assays. The DPPH assay will determine the sample's ability to scavenge DPPH free radicals, while the ABTS assay will measure its effectiveness in neutralizing ABTS free radicals. By comparing the antioxidant activity of the nanosuspension with that of conventional herbal extracts using these two methods, this research aims to provide deeper insight into the therapeutic potential of the new formulation.

This study is expected to contribute to the advancement of more efficient and effective herbal medicines. By employing nasuspension technology, it aims to enhance the bioavailability of active compounds, overcome solubility issues associated with poorly soluble substances, and improve therapeutic effectiveness. Ultimately, this approach has the potential to optimize herbal treatments and lead to better health outcomes.

2. EXPERIMENTAL SECTION

2.1 Materials

The materials used in this study include chitosan, sodium alginate, sodium tripolyphosphate, ethanol (p.a.), glacial acetic acid, lead acetate, purified water (aquadest), Tween 80, DPPH, quercetin, methanol (p.a.), 2,2'-azino-bis(3-ethylbenzothiazoline-6-sulfonic acid) (ABTS), Trolox, dimethyl sulfoxide (DMSO) 100% solvent, aluminum foil, potassium persulfate ($K_2S_2O_3$), and various solvents such as methanol, ethanol, and purified water. All chemicals were sourced from Merck or Bratachem as specified.

2.2 Instrumentation

Particle Size Analyzer (Dynamic Light Scattering, Malvern), Zetasizer (Malvern, UK) for zeta potential, UV-Vis Spectrophotometer, Transmission Electron Microscope (TEM), Fourier Transform Infrared Spectrophotometer (FT-IR, Shimadzu FT-IR 8300), Differential Scanning Calorimeter (DSC, Shimadzu DSC-60), Centrifuge, Analytical balance, Magnetic stirrer, vortex, pH meter, glassware.

2.3 Methods

2.3.1 Phytomchemical Screening

The alkaloid test involved adding 1 mL of 2 N hydrochloric acid and 9 mL of heated distilled water to the sample, followed by the addition of Dragendorff's reagent, which produced an orange to crimson precipitate. When Mayer's reagent was added, a yellowish-white precipitate formed, while Wagner's reagent resulted in a brown precipitate. For the flavonoid test, 1 mL of amyl alcohol, 1 mL of concentrated hydrochloric acid, and magnesium powder were combined with the sample. This procedure produced a red, yellow, or greenish-brown coloration in the amyl alcohol layer. The phenolic test was carried out by adding 1% ferric chloride ($FeCl_3$), which resulted in color changes ranging from green to purple, blue, or black. For the saponin test, 10 mL of heated water and one drop of 2 N

Table 1. Nanosuspension Formula Containing *Apium graveolens*, *Centella asiatica*, and *Orthosiphon stamineus* Extract

Run	Factor 1 A : Tween 80 (grams)	Factor 2 B : Chitosan (mL)	Factor 3 C : Na-TPP (mL)
1	3	25	10
2	3	25	5
3	3	20	5
4	6	25	5
5	6	25	10
6	6	20	10
7	6	20	5
8	6	20	10

hydrochloric acid were added, producing a stable foam. Lastly, the steroid and triterpenoid assay involved the addition of 2 mL of chloroform, 0.5 mL of anhydrous acetic acid, and a drop of concentrated sulfuric acid, where a green color indicated steroids and blue or red hues indicated triterpenoids (Syukur et al., 2023).

2.3.2 Total of Flavonoid

Preparation of the Standard Curve: Accurately weigh up to 10 mg of quercetin and transfer it into a 25 mL volumetric flask. Dissolve the quercetin in ethanol, sonicate the solution, and then fill the flask to the mark with ethanol. Transfer this solution to a cuvette and measure its absorbance within the wavelength range of 400–600 nm. Determination of Flavonoid Content: Weigh the sample and place it into a conical flask. Add 2 mL of ethanol, then vortex and sonicate the mixture for one hour. Afterward, centrifuge the sample, transfer the supernatant to a 10 mL graduated flask, and repeat the extraction process to ensure thorough flavonoid extraction (Sulastri et al., 2018)

2.3.3 Formula Design

The optimization of the nanosuspension formulation was carried out using a full factorial design with two levels, implemented through the Design-Expert®version 13 software. Three independent variables were selected as key factors: the concentrations of Tween 80 (A), chitosan (B), and sodium tripolyphosphate (NaTPP) (C). Upper and lower limits were set to define the ratios of chitosan, NaTPP, and Tween 80, resulting in the creation of eight different test formulations. Specifically, chitosan was tested at concentrations of 20 and 25 mL, NaTPP at 5 and 10 mL, and Tween 80 at 3 and 6 grams (Nafisa et al., 2023). The design of the nanosuspension formulation is presented in Table 1.

2.3.4 Preparation of Nanosuspension

Two hundred milligrams of chitosan were dissolved in 100 mL of purified water acidified with 1% acetic acid. Separately, 100 milligrams of sodium tripolyphosphate (Na-TPP) were dissolved in 100 mL of purified water. Concentrated extracts of *Apium graveolens, Centella asiatica,* and *Orthosiphon stamineus* were mixed thoroughly with the surfactant polysorbate 80 in a mortar until completely dissolved. The mixture was then transferred to a glass beaker and stirred at 1200 rpm for 10 minutes. Subsequently, a 0.2% chitosan solution was added slowly while maintaining continuous stirring for 15 minutes. Following this, a 0.1% Na-TPP solution was gradually introduced and the mixture was stirred for an additional 60 minutes. he procedure for preparing the nanosuspension can be seen in Figure 1 (Arifin et al., 2022; Nafisa et al., 2023).

2.3.5 Preparation of Nanosuspension

Two hundred milligrams of chitosan were dissolved in 100 mL of purified water acidified with 1% acetic acid. Separately, 100 milligrams of sodium tripolyphosphate (Na-TPP) were dissolved in 100 mL of purified water. Concentrated extracts of *Apium graveolens, Centella asiatica,* and *Orthosiphon stamineus* were mixed thoroughly with the surfactant polysorbate 80 in a mortar until completely dissolved. The mixture was then transferred to a glass beaker and stirred at 1200 rpm for 10 minutes. Subsequently, a 0.2% chitosan solution was added slowly while maintaining continuous stirring for 15 minutes. Following this, a 0.1% Na-TPP solution was gradually introduced and the mixture was stirred for an additional 60 minutes. he procedure for preparing the nanosuspension can be seen in Figure 1 (Arifin et al., 2022; Nafisa et al., 2023).

2.3.6 Characteristic of nanosuspension

Particle size and distribution were examined using a Particle Size Analyzer (PSA) based on Dynamic Light Scattering (DLS) technology with a Malvern instrument. Prior to measurement, 100 μL of the nanoemulsion sample was diluted in 10 mL of distilled water to achieve an optimal scattering intensity. The DLS method provided both the particle diameter and the polydispersity index, which serve as indicators of nanoparticle size distribution. These parameters were determined from three measurements taken at a 173° scattering angle using a polystyrene cuvette, with all analyses performed at a controlled temperature of 25°C. Zeta potential characterization was performed using a Malvern Zetasizer (model 1203893) to assess

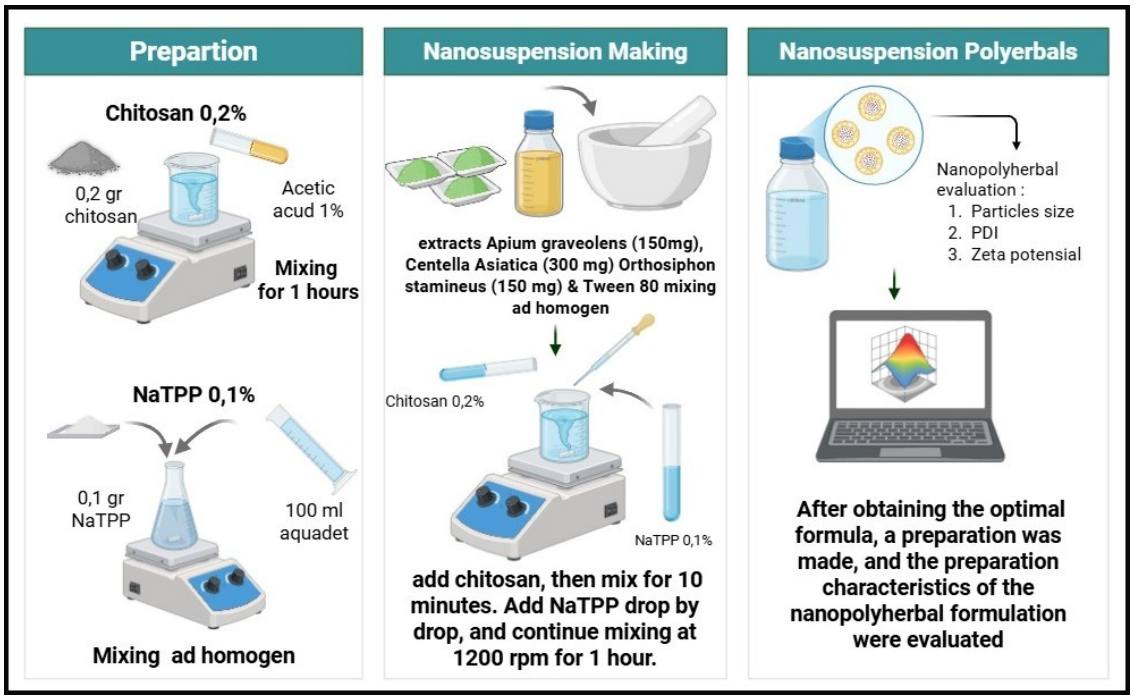

Figure 1. Procedure for the Formulation of Nanopolyherbal Preparations

the electrical charge properties of the nanoencapsulation. Zeta potential serves as an indicator of the stability of a dispersion system. The measurement was conducted by evaluating the electrophoretic mobility of the particles. For analysis, 100 microliters of the sample were diluted in 10 mL of distilled water and placed into a cuvette equipped with electrodes (Astuti et al., 2025)

2.3.7 Determination of Optimum Formula

The optimal formulation was determined using the two-level factorial design approach implemented through the Design-Expert 13 software. Based on the concentration variations specified by the software, eight different formulations were developed. Each formulation was then evaluated for particle size, polydispersity index (PDI), and zeta potential. Following the recommendation of Narukulla et al. (2024), these test results were used as response variables to identify the best-performing formula. The optimal formulation corresponds to the highest desirability value. A desirability value approaching 1 indicates that the response is very close to the target specification.

2.3.8 Characteristics of Optimum Formula Nanosuspension

Particle size, polydispersity index (PDI), and zeta potential were measured using a dynamic light scattering particle size analyzer (Zetasizer ZS90, Nanoseries, Malvern®, UK). Prior to analysis, all samples were diluted 1,000-fold with demineralized water and placed in quartz cuvettes, following the procedure described by Godge et al. (2020). Measurements were conducted at 25°C with a scattering angle of 90°. Each measurement was performed in triplicate, and the mean value was reported.

Drug-excipient interactions and crystallinity inside of the formulation were investigated utilizing Fourier Transform Infrared Spectroscopy (FT-IR) by a Shimadzu FT-IR 8300 spectrophotometer and Differential Scanning Calorimetry (DSC) by a Shimadzu DSC-60, over a wavelength range of 4000–400 cm^{-1}. Particle morphology was tested by Transmission Electron Microscopy (TEM). For this, a diluted nanosuspension sample was placed onto a TEM grid and allowed to rest for one minute to ensure uniform particle distribution. Excess liquid was then omitd by filter paper, and the grid was dried before detailed size and morphology analysis under the TEM (Astuti et al., 2025; Pınar et al., 2023).

2.3.9 Stability Test

The stability of the optimized polyherbal nanosuspension was systematically assessed over a 30-day duration under three storage conditions: ambient (25°C), refrigerated (4°C), and accelerated (40°C). Samples were collected at designated intervals (0, 7, 14, 21, and 30 days) and analyzed for particle size, polydispersity index (PDI), and zeta potential utilizing a Malvern Zetasizer (ZS90, UK) following a 1:1000 dilution with distilled water. The pH of the nanosuspension was evaluated using a digital pH meter (Mettler Toledo, Germany). Concurrently, ocular examinations were conducted to detect any changes in color, odor, or phase separation. All measurements were performed in triplicate, and the data were expressed as mean ± standard deviation (SD). The results were employed to evaluate the physical and colloidal stability of the formulation, revealing vital details about its durability and suitability for extended storage and potential therapeutic application (Jahan

et al., 2023).

2.4 DPPH Method

DPPH 50 ppm is made by dissolving 5 mg DPPH Crystals in 100 mL methanol (Cruz-Casas et al., 2023). To determine the maximum absorption wavelength of DPPH, 1 mL of a 50 ppm DPPH solution was mixed with 3 mL of methanol in a test tube and thoroughly homogenized. The mixture was then incubated at room temperature for 30 minutes. The optimum wavelength was then identified by measuring absorbance within the range of 510 to 525 nm. For sample preparation, 25 mg of each sample-both the polyherbal combination and the polyherbal nanoencapsulation-was accurately weighed and dissolved in 25 mL of methanol in a volumetric flask to obtain a 100 ppm stock solution. From this stock, a series of diluted solutions with concentrations of 10, 15, 20, 25, and 30 ppm were prepared. A quercetin solution was prepared to serve as a reference standard. Precisely 5 mg of quercetin was weighed and dissolved in methanol, then transferred to a 50 mL volumetric flask and diluted to volume with methanol to yield a 100 ppm stock solution. From this stock, a series of dilutions were prepared at concentrations of 1, 2, 3, 4, and 5 ppm. Absorbance measurements were performed using a UV-Vis spectrophotometer. For each test, 1 mL of the sample or standard solution was mixed with 1 mL of 100 ppm DPPH solution and 2 mL of methanol in a test tube, followed by thorough mixing until homogeneous. The mixtures were incubated at room temperature for 30 minutes before measuring absorbance at the previously determined optimal wavelength for DPPH. All experiments were conducted in triplicate (Pakki et al., 2020; Susanti et al., 2023).

2.4.1 ABTS Method

The ABTS solution was prepared by accurately weighing 19.2 mg of ABTS and dissolving it in 5 mL of distilled water, followed by thorough mixing. The solution was then protected from light by covering it with aluminum foil. Separately, a potassium persulfate ($K_2S_2O_8$) solution was prepared by dissolving 37.8 mg of $K_2S_2O_8$ in 1 mL of distilled water and mixing well to ensure complete dissolution. An ABTS stock solution was prepared by mixing 88 μL of the potassium persulfate ($K_2S_2O_8$) solution with the ABTS solution, followed by thorough homogenization. This mixture was then incubated at room temperature for 18 to 22 hours. After incubation, 1 mL of the stock solution was transferred into a 50 mL tube and homogenized once more before use. The absorbance of the solution, which should not exceed 0.7, was measured by adding 300 μL of media blank into a 96-well plate, starting from the highest to the lowest concentration. Measurements were taken at a wavelength of 630 nm, with all concentrations tested in triplicate. The ABTS solution was transferred to a reservoir, and 290 µL was dispensed into each well of the plate containing the standard solutions, blanks (solvent and ABTS), and samples using a multichannel pipette. The plate was then covered with aluminum foil and incubated in the dark at room temperature for 6 minutes. Following incubation, the absorbance was recorded using a microplate reader at 630 nm over 30 seconds, with medium shaking applied.

A 1.000 ppm Trolox standard solution was prepared by accurately weighing 10 mg of Trolox, dissolving it in 10 mL of distilled water, and mixing thoroughly. From this stock, a series of concentrations was created at 3.91, 15.63, 31.25, 62.50, 125, and 150 ppm. A 100.000 ppm sample solution was prepared by dissolving 100 mg of the sample in 1 mL of DMSO, followed by vortex homogenization. Subsequently, concentration series were prepared for each sample type: for the polyherbal extract, concentrations of 781.25, 1.562.50, 6.250, 12.500, and 25.000 ppm were made; for the nano polyherbal sample, concentrations of 1.56, 3.13, 6.25, 12.5, 25, and 100 ppm were prepared (Chaves et al., 2020; Lukman et al., 2024)

2.4.2 Data Analysis

The mean ± standard deviation (SD) of three distinct measurements was employed to present the characterization data of the nanosuspensions, encompassing particle size, polydispersity index (PDI), and zeta potential. One-way ANOVA and Tukey's post-hoc test were employed to assess differences among formulations, utilizing a significance threshold of $p < 0.05$ Formulation optimization was conducted utilizing a factorial design in Design-Expert®13 software, employing a response surface methodology to evaluate the impact of Tween 80, chitosan, and Na-TPP concentrations on particle characteristics. The desirability function was employed to determine the optimal formulation; formulas with values near 1 are deemed the most suitable. The DPPH and ABTS assays were employed to assess antioxidant activity, with the percentage inhibition calculated as follows:

$$\% \text{ Inhibition} = \frac{\text{Absorbance Control} - \text{Absorbance Sample}}{\text{Absorbance Control}} \times 100 \quad (1)$$

The linear regression of sample concentration vs. percentage inhibition was used to calculate the IC_50 value, which is the concentration needed to inhibit 50% of free radicals. A one-way ANOVA with $p < 0.05$ was used to examine the differences between the nanosuspension and traditional herbal extracts, and antioxidant results were also presented as mean ± SD from three repetitions. Response surface plots were used to show how formulation variables affected the properties of the nanosuspension, and OriginPro was used to depict the particle size distribution, PDI, zeta potential, and antioxidant activity curves.

3. RESULTS AND DISCUSSION

3.1 Phytochemical Screening

Identifying the phytochemical compounds in the extracts of *Apium graveolens, Centella asiatica,* and *Orthosiphon stamineus*

is a crucial initial step for assessing their potential biological, medicinal, and technical applications (Kandasamy et al., 2023) Each extract was examined for the presence of key phytochemical groups, including alkaloids, flavonoids, tannins, saponins, steroids, and terpenoids. The qualitative phytochemical analysis results are summarized in Table 2 for the extracts of *Apium graveolens, Centella asiatica,* and *Orthosiphon stamineus*. The celery extract contains alkaloids, flavonoids, tannins, saponins, and terpenoids, while the extracts from *Centella asiatica* and *Orthosiphon stamineus* contain alkaloids, flavonoids, tannins, saponins, steroids, and terpenoids.

Emad et al. (2022) indicates that the extract of *Apium graveolens* leaves has alkaloids, flavonoids, tannins, saponins, and terpenoids. S et al. (2017) identified that the extract of *Centella asiatica* included alkaloids, flavonoids, glycosides, phenols, saponins, steroids, tannins, and terpenoids. Sivakumar and Jeganathan (2018) report that *Orthosiphon stamineus* extract comprises alkaloids, flavonoids, steroids, terpenoids, tannins, and saponins. Preliminary phytochemical screening is valuable for examining bioactive compounds and may facilitate medication development and discovery (Dubale et al., 2023).

Table 2. Phytochemical Screening Test

Compounds	*Apium Graveolens*	*Centella asiatica*	*Orthosiphon stamineus*
Flavonoid	+	+	+
Alkaloid	+	+	+
Tannins	+	+	+
Saponin	+	+	+
Steroid	-	+	+
Terpenoid	+	+	+

The total flavonoid content in extracts of *Apium graveolens, Centella asiatica,* and *Orthosiphon stamineus* was measured using a colorimetric assay based on the aluminum chloride ($AlCl_3$) method, with quercetin serving as the reference standard. This technique quantifies flavonoids by detecting the formation of a yellow complex that occurs when $AlCl_3$ reacts with the keto and hydroxyl groups found in flavones and flavonols. The data obtained from this assay are presented in Table 3, showing the flavonoid content for each plant extract. The values are expressed in terms of quercetin equivalents (QE), providing a clear comparison of the flavonoid levels among the extracts. The total flavonoid content in extracts of *Apium graveolens, Centella asiatica* and *Orthosiphon stamineus* was measured using a colorimetric assay based on the aluminum chloride ($AlCl_3$) method, with quercetin serving as the reference standard. This technique quantifies flavonoids by detecting the formation of a yellow complex that occurs when $AlCl_3$ reacts with the keto and hydroxyl groups found in flavones and flavonols. (Sultana et al., 2024; Syukur et al., 2023). The flavonoid concentration in *Orthosiphon stamineus* extract was 3.216 mg QE per gram, surpassing the results of Hizar et al. (2024) and Ho et al. (2014), which reported flavonoid levels of 74.09 mg/100 g and 45.00 mg/100 g, respectively. The polyherbal extract exhibited a heightened flavonoid concentration of 6.18 mg QE per gram, likely due to the synergistic interactions among various plant extracts that enhance the extraction and stability of flavonoids (Hassanpour and Doroudi, 2023). In contrast, the nanopolyherbal extract, employing nanotechnology, demonstrated a diminished flavonoid concentration of 1.155 mg QE per gram. The reduced concentration may stem from the intricacies of nanoparticle formulations, where surfactants and stabilizers, while crucial for stabilization, could interact with flavonoids and impair encapsulation efficacy, leading to degradation or loss of active compounds (Puspadewi et al., 2025; Zhou et al., 2023). The total flavonoid concentration in plant extracts exhibits a robust association with antioxidant action (Lukman et al., 2024). Flavonoids function as free radical scavengers by donating electrons to neutralize these harmful molecules, thereby reducing oxidative damage to cells. A higher flavonoid content is generally associated with greater antioxidant potential, which can help protect the body against oxidative stress and various related diseases (Hassanpour and Doroudi, 2023).

Table 3. Total Flavonoids

Sample	Result	Unit
Apium graveolens	1.850±0.046	mg QE/g extract
Centella asiatica	0.957±0.046	mg QE/g extract
Orthosipon stamineus	3.216±0.046	mg QE/g extract
Combination of Polyherbal	6.18 ± 0.071	mg QE/g extract
Nanopolyherbal	1.155± 0.025	mg QE/g extract

3.2 Formula Design

The optimization of nanosuspensions containing extracts of celery, cat's whiskers, and centella was carried out using the Design of Experiment (DoE) approach, facilitated by Design Expert (DX) software version 13. A factorial design was selected for the DoE, which uses regression equations to model the relationships between response variables and one or more independent factors (Jankovic and Chaudhary, 2021). The experimental design of this study included three independent variables as main factors: Tween 80 concentration (A), chitosan (B), and NaTPP (C). The primary response variables assessed in the nanosuspension formulation were particle size diameter (R1), polydispersity index (PDI, R2), and zeta potential (R3). Comprehensive data from the factorial design are presented in Table 4. Particle size ranged from 131 nm to 292 nm, PDI values varied between 0.62 and 0.99, and zeta potential measurements spanned from -22.74 to -32.24 mV. The smallest particle size and lowest polydispersity index (PDI) were observed in run 5, which used 6 grams of Tween 80. 25 mL of chitosan, and 10 mL of Na-TPP. This result indicates a more uniform particle size distribution compared to the other formulations tested. This matches the study by Heinz et al. (2017) which showed that using the right surfactants can improve the

Figure 2. Product of Eight Formula

Table 4. Results of Particle Size, PDI, and Zeta Potential Tests on Nanosuspensions

Run	Tween 80 (gr)	Chitosan (mL)	Na-TPP (mL)	Particle size	PDI	Zeta potensial
1	3	25	10	277±6.24	0.99±0.004	-26.16±0.46
2	3	25	5	204±3.60	0.69±0.005	-25.25±0.09
3	3	20	5	234±3.46	0.88±0.05	-22.78±0.025
4	6	25	5	292±2	0.98±0.005	-22.74±0.1
5	6	25	10	131±2	0.62±0.033	-23.38±0.03
6	3	20	10	285±4.58	0.89±0.043	-27.96±0.06
7	6	20	5	218±5.57	0.68±0.03	-27.84±0.147
8	6	20	10	245±8	0.77±0.04	-32.24±0.034

stability and size of particles in nanoparticle systems. The eight nanosuspension formulations are depicted in Figure 2.

3.2.1 Evaluation of Particle Size Diameter Response (R1)

Achieving particle sizes within the nanometer range is essential in the production of polymeric nanoparticles, making particle size a crucial parameter. Analysis of the residuals indicates that they generally follow a normal distribution, with only slight deviations. This is supported by the plot, where most data points align closely along a straight line, suggesting normality despite minor departures. Therefore, the conditions for conducting the ANOVA test are met. The detailed results of the statistical analysis for particle size are presented in Table 5 and Figure 3.

The ANOVA analysis for particle size indicated that the model was not statistically significant, with an F-value of 0.43 and a p-value of 0.82 (p >0.05). This suggests that neither the individual independent variables-Tween 80, chitosan, and NaTPP-nor their interactions had a meaningful effect on particle size. The results also showed that the p-values for each factor exceeded 0.05, confirming that variations in the concentrations of these components did not produce significant changes in particle size. The lack of significance in the model may be due to the exclusion of other influential factors or variations not accounted for in the tested variables (Akram and Garud, 2021).

3.2.2 Evaluation of Polydispersity Index Response (R2)

The polydispersity index (PDI) reflects the variability in particle sizes within a sample; for polymeric nanoparticles, this refers to the particle diameter measured in nanometers. Lower PDI values, approaching zero, indicate a more uniform and well-dispersed particle size distribution (Aluani et al., 2017; Maity et al., 2017). The evaluation of the PDI response indicates that the data follow a normal distribution Figure 4, as evidenced by the data points clustering closely around a straight line according to the observed response values. The ANOVA results for the PDI response revealed that the overall model was not statistically significant (F = 135.81, P = 0.0656), suggesting it did not adequately account for the variations in PDI. The detailed results of the statistical analysis for particle size are presented in Table 6. However, certain individual factors showed greater significance within the analysis. Factor A (Tween 80) significantly impacted PDI, as indicated by a P-value of 0.0255, demonstrating that variations in Tween 80 substantially influenced PDI changes. Although Factor B (chitosan) and the interaction between A and B showed relatively high F-values, their P-value of 0.0656 suggested they were only marginally significant. In contrast, Factor C (NaTPP) and the interactions AC and BC exhibited high P-values ranging from 0.3440 to 0.7952, indicating no significant effect on PDI. Therefore, Tween 80 was identified as the primary factor affecting PDI, while the other factors and their interactions did not reach statistical significance within the accepted threshold.

Table 5. ANOVA Results for Particles Size Response

Parameter	Sum of squares	df	Mean square	F-value	P-value	Model status
Model	2.6176	6	4362.67	87.25	0.0818	not significant
A-Tween 80	5304.50	1	5304.50	106.09	0.0616	
B-Chitosan	968	1	968	19.36	0.1423	
C-NaTPP	1200.50	1	1200.50	24.01	0.1282	
AB	1404.50	1	1404.50	28.09	0.1187	
AC	8978.00	1	8978.00	179.56	0.0474	
BC	8320.50	1	8320.50	166.41	0.0493	
Residual	50	1	50			
Cor Total	26226.00	7				

Table 6. ANOVA Results for PDI Response

Parameter	Sum of squares	df	Mean square	F-value	P-value	Model status
Model	0.0917	6	0.0153	135.81	0.0656	not significant
A-Tween 80	0.0703	1	0.0703	625.00	0.0255	
B-chitosan	0.0105	1	0.0105	93.44	0.0656	
C-NaTPP	0.0000	1	0.0000	0.1111	0.7952	
AB	0.0105	1	0.0105	93.44	0.0656	
AC	0.0003	1	0.0003	2.78	0.3440	
BC	0.0000	1	0.0000	0.1111	0.7952	
Residual	0.0001	1	0.0001			
Cor Total	0.0918	7				

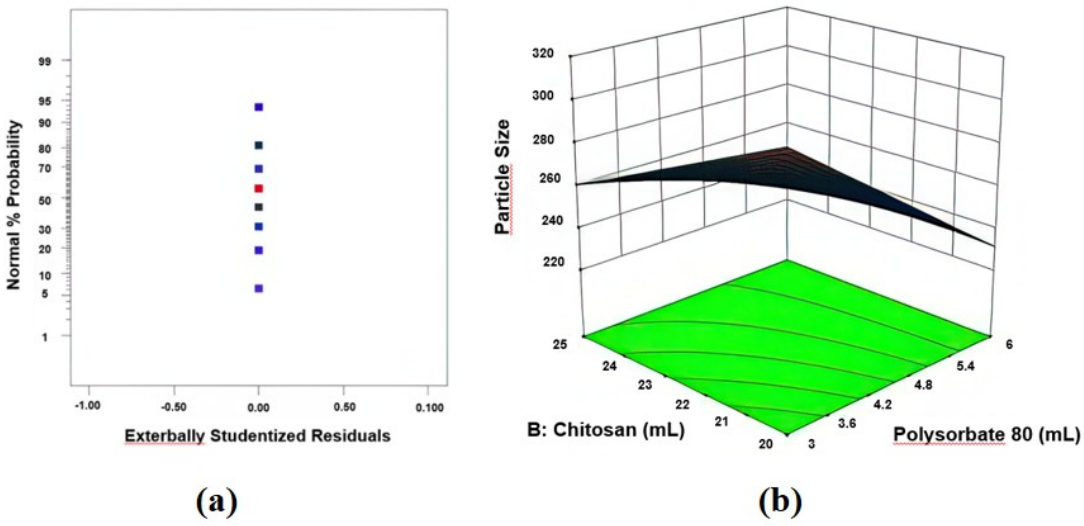

Figure 3. Normal Plot of Recidual, (b) Surface of Particle Size Nanosuspension

3.2.3 Evaluation of Zeta Potential Response (R3)

The ANOVA analysis of the zeta potential response indicates that the model is statistically significant, with a p-value of 0.0391. This finding suggests that the variables included in the model meaningfully influence zeta potential. Factor A (Tween 80) showed a p-value of 0.0797, indicating it does not have a significant effect on zeta potential, as this value exceeds the 0.05 threshold. In contrast, Factor B (chitosan) and Factor C (Na-TPP) demonstrated significant effects, with p-values of 0.0244 and 0.0292 respectively, highlighting their important roles in controlling nanoparticle stability.

The inclusion of Tween 80, chitosan, and sodium tripolyph osphate (Na TPP) in nanoparticle synthesis affects the zeta potential, reflecting the electrostatic stability of the system. Tween 80 enhances particle dispersion by lowering surface tension, while positively charged chitosan contributes to stability

Table 7. ANOVA Results for Zeta Potential Response

Parameter	Sum of squares	df	Mean square	F-value	P-value	Model status
Model	74.57	6	12.43	382.24	0.0391	significant
A-Tween 80	2.05	1	2.05	63.06	0.0797	
B-Chitosan	22.08	1	22.08	679.06	0.0244	
C-NaTPP	15.48	1	15.48	476.27	0.0292	
AB	26.75	1	26.75	822.90	0.0222	
AC	0.1378	1	0.1378	4.24	0.2879	
BC	8.06	1	8.06	247.91	0.0404	
Residual	0.0325	1	0.0325			
Cor Total	74.60	7				

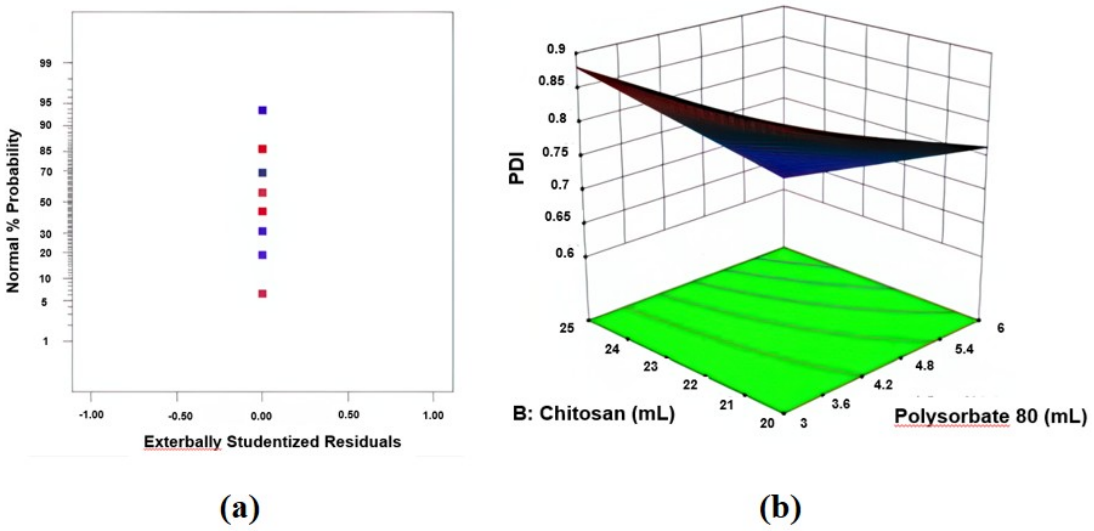

Figure 4. (a). Normal Plot of Recidual, (b) Surface of Zeta Potential Nanosuspension

through its interaction with negatively charged particles. Na TPP acts as a crosslinking agent, organizing the polymer network. Together, these components optimize zeta potential values, improve nanoparticle stability, and reduce aggregation-key factors for effective drug delivery and applications in nanomedicine (Kaur et al., 2021; Scolari et al., 2019).

The interaction between Tween 80 and chitosan (AB) was found to be statistically significant, with a p-value of 0.0222, indicating a meaningful impact on the zeta potential. In contrast, the combined effect of Tween 80 and Na-TPP (AC) was not significant, as shown by a p-value of 0.2879, suggesting their joint influence on zeta potential is limited. Meanwhile, the interaction between chitosan and Na-TPP (BC) demonstrated significance (p = 0.0404), implying this interaction plays an important role in modulating the zeta potential. This effect is likely driven by electrostatic interactions between chitosan and Na-TPP, which enhance particle stability. The results of the ANOVA analysis for the PDI response can be seen in Table 7 while the normal plot of residuals and the 3D surface plot for zeta potential are presented in Figure 5.

3.3 Statistical Analysis of All Responses (R1, R2, and R3)

Statistical Analysis of All Responses is presented in Table 8. The statistical analysis reveals that the developed models R1, R2, and R3 demonstrate excellent fit and reliability. Specifically, the particle size model shows an R^2 of 0.9981, an adjusted R^2 of 0.9867, and a predicted R^2 of 0.8780, indicating that the model accounts for nearly all variability in the data while maintaining strong predictive power. Although the predicted R^2 is slightly lower than the adjusted R^2, the difference is within an acceptable range-less than 0.2-suggesting that the model is robust and reliable when applied to new data. The PDI response shows strong consistency across parameters, reflected by an R^2 of 0.9988, an adjusted R^2 of 0.9914, and a predicted R^2 of 0.9216, indicating a reliable and accurate predictive model. Similarly, the zeta potential displays an even higher R^2 value of 0.9996, with both the adjusted and predicted R^2 values reaching 0.9996 and 0.9721, respectively, highlighting the model's excellent performance. The small difference between the predicted R^2 and the original R^2-less than 0.2-indicates that the model possesses strong predictive power and impressive stability. These results collectively suggest that the model

Table 8. Statistical Analysis Results of Factorial Design on All Responses

	Parameter						
Respon	SD	Mean	CV %	R^2 value	Adjusted R^2	Predicted R^2	Adequate precision
R1	7.07	259.50	31.49	0.9981	0.9867	0.8780	30.9931
R2	0.0106	0.7863	1.35	0.9988	0.9914	0.9216	27.4654
R3	0.1803	-26.04	0.6923	0.9996	0.9996	0.9721	56.3241

performs reliably in estimating the three response variables. The close alignment between predicted and original R^2 values further implies that the model is not overfitted and is capable of generalizing well to new, unseen data.

3.4 Determination of the Optimal Formula and Formula Verification

Based on the analysis of experimental data and factorial design, the optimal formulation for the polyherbals extract nanosuspension was identified. This formulation consists of 6 g of Tween 80, 21 mL of chitosan, and 10 mL of NaTPP. The desirability score of 0.7-relatively close to the maximum value of 1-indicates a strong alignment between the predicted outcomes and the experimental results. This formulation is expected to produce nanoparticles with a size of approximately 227 nm, a polydispersity index (PDI) of 0.721, and a zeta potential of -30.048, reflecting favorable characteristics for nanosuspension stability and performance.

The optimal formulation was validated using point prediction analysis, incorporating both a 95% confidence interval (CI) and a 95% prediction interval (PI). The CI reflects the expected range for the mean of repeated measurements at a 95% confidence level, while the PI represents the range within which individual predicted values are likely to fall, also with 95% confidence (Weissman and Anderson, 2015). The predicted optimal particle size was 227 nm, while the experimentally observed value was 186 nm. The 95% confidence interval (CI) for the mean ranged from 158.32 nm to 297.04 nm, and the 95% prediction interval (PI) extended more broadly, from -97.25 nm to 552.61 nm. This wide prediction interval may reflect variability in the formulation process, which could affect the consistency of the resulting particle size (Ahmadi Tehrani et al., 2019). Determination of the Optimal Formula and Formula Verification is presented in Table 9.

3.5 Characterization Results of Particles Size, Polydispersity Index, and Zeta Potential of Optimum Nanosuspension Formula

The particle size diameter of the optimized formulation was measured at 220 ± 11.57 nm, which falls well within the accepted nanoparticle range of 1 to 1000 nm. The results suggest that the components-Tween 80, chitosan, and NaTPP-play a significant role in determining the final particle size. The characteristics of the optimized formulation are presented in Table 10. The measurement process aligns with analytical standards defined by Dynamic Light Scattering–Particle Size Analysis (DLS-PSA). From a theoretical perspective, reducing particle size to the nanoscale can improve the bioavailability of active compounds. Smaller particles enhance absorption within the body and help regulate the release rate of active ingredients from the polymeric nanoparticle delivery system (Pereira et al., 2018).

The polydispersity index (PDI) is closely related to particle size, serving as a key indicator of particle size distribution within a formulation. In the optimized formulation, the PDI was measured at 0.59±0.06. This value suggests a broad size distribution, as a PDI ≥ 0.3 typically reflects lower homogeneity among particles. A higher PDI (≥ 0.5) indicates significant variation in particle sizes, pointing to a non-uniform distribution. Conversely, a PDI value approaching zero implies a high degree of uniformity, with particles exhibiting relatively consistent sizes throughout the sample (Danaei et al., 2018). The uniformity of particle distribution, or homogeneity, influences the stability of the created nanopolymeric system and has been shown to enhance bioavailability (Li et al., 2016).

Zeta potential refers to the possible difference between the surfaces of particles. The zeta potential value is related to the push away force between nearby particles that have the same charge in the mixture (Liu et al., 2020). Particles or molecules with a high zeta potential tend to experience strong repulsive forces, which help prevent aggregation and promote greater stability in dispersion. In contrast, a low zeta potential allows attractive forces to dominate, increasing the likelihood of particle flocculation and eventual breakdown of the dispersion. Therefore, a high zeta potential—whether positive or negative-is generally desirable in formulations, as it indicates a stable colloidal system (Németh et al., 2022).

The stability of the polyherbals extract nanosuspension was evaluated through zeta potential analysis. A higher absolute value of zeta potential-regardless of whether it is positive or negative-indicates that repulsive forces between particles are dominant over attractive forces, thereby reducing the likelihood of aggregation. The predicted zeta potential was -30.08 mV, with a 95% confidence interval (CI) ranging from -31.85 to -28.31 mV, and a wider 95% prediction interval (PI) spanning from -38.37 to -21.79 mV. These values suggest a stable formulation with minimal risk of particle flocculation.

The drug content of the nanosuspension was evaluated using sinensetin as the marker compound from *Orthosiphon stamineus*. The results (Table 11) demonstrated that the drug content values from three replicates ranged from 95.90% to 98.24%, with a mean of 97.20 ± 1.18% (n = 3). The observed values closely matched the theoretical content, indicating that

Table 9. Prediction Results and Verification Range of the Optimal Formula

Respon	Prediction	Observation	95% CI		95% PI	
			Lower	Upper	Lower	Upper
Particle Size	227	220 ± 11.57	158.32	297.04	-97.2484	552.606
PDI	0.72	0.59±0.06	0.62	0.83	0.233659	1.20844
Zeta potential	-30.08	-28.27±0.37	-31.85	-28.314	-38.3692	-21.798

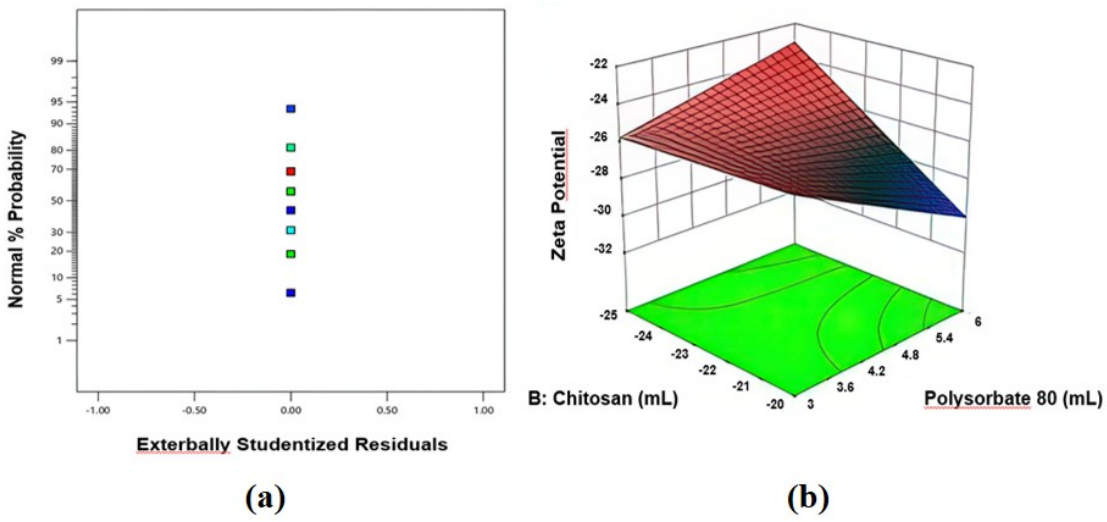

Figure 5. (a). Normal Plot of Recidual, (b) Surface of Zeta Potential Nanosuspension

Table 10. Characterization of the Optimal Nanosuspension Formula

Nanopolyherbal	Particle size (nm)	Polydispersity index	Zeta potential (mV)
Replication 1	236	0.55	-27.77
Replication 2	215	0.68	-28.66
Replication 3	209	0.54	-28.38
Mean ± SD	220 ± 11.57	0.59±0.06	- 28.27±0.37

Table 11. Drug Content of Sinensetin in Polyherbal Nanosuspension

Formula	Theoretical drug content (mg)	Measured drug content (mg)	Drug content (%)
Replicate 1	50.00	48.73	97.46
Replicate 2	50.00	47.95	95.90
Replicate 3	50.00	49.12	98.24
Mean ± SD			97.20 ± 1.18

the formulation method effectively preserved the majority of the active chemical without significant degradation or loss during the production of the nanosuspension. The increased drug content results demonstrate the formulation approach's stability and reproducibility, along with the nanosuspension system's ability to maintain the integrity of the marker compound. The consistency among replicate measurements further confirms that the active chemical concentration stayed within the expected range. These findings align with prior research indicating that drug content values exceeding 90% are generally deemed acceptable for maintaining formulation quality and therapeutic efficacy (Aldeeb et al., 2025). Thus, the nanosuspension developed in this study is considered pharmaceutically sound and suitable for further pharmacological evaluation.

The results of the stability test for the nanopolyherbal formulation-including particle size, polydispersity index (PDI), and zeta potential-are presented in Table 12. The stability tests showed no changes in color, with sediment remaining consistent throughout the storage period. Particle size gradually increased from day 1 to day 60, likely due to agglomerate formation over time. Nevertheless, the polydispersity index (PDI) remained within an acceptable range, and although the zeta potential exhibited a slight decline, it remained sufficiently high to maintain strong repulsive forces between particles, which are essential for sustaining the formulation's stability. The results match what Fan et al. (2012) found, showing that when stored at low temperatures between 10°C and 25°C, the size of the nanokitosan particles stayed small. Additionally, the research

by López-León et al. (2005) showed that at -10°C, the chitosan nanoparticle solution was unstable, but at 5°C and 25°C, the size of the particles grew significantly on the 7th and 15th days.

Transmission Electron Microscopy (TEM) analysis, shown in Figure 6, reveals that the particles in the nanosuspension are spherical and exhibit a small, uniform size distribution. With an approximate particle size of 184 nm, they fall within the ideal nanometer range for nanosuspensions, supporting enhanced solubility, controlled release of active compounds, and increased bioavailability. The consistent particle shape also indicates that the surfactants effectively stabilize the particles and prevent aggregation, potentially improving the overall distribution of active ingredients throughout the nanosuspension.

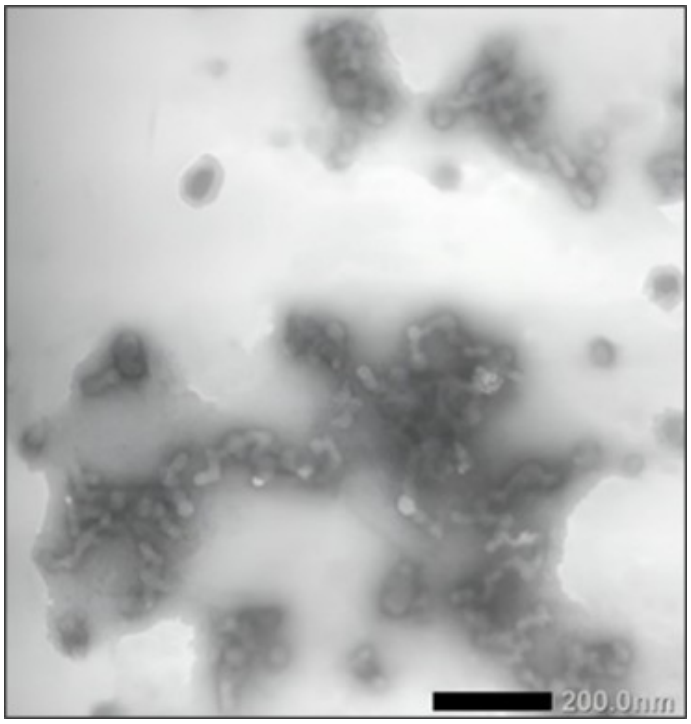

Figure 6. Morphological Results of Nanopolyherbal using TEM

We conducted the subsequent characterization test using FTIR spectroscopy. FTIR is a rapid and precise technique that yields information regarding the functional groups present in the sample. This is a principal analytical technique favored for its screening efficacy, rapidity, and cost-effectiveness. People refer to this technique as a "molecular fingerprint" method (Kumar and Pandey, 2013). FTIR analysis facilitates the identification of functional groups in plant extracts and nanopolyherbal formulations. As previously stated, extracts of *Apium graveolens, Centella asiatica,* and *Orthosiphon stamineus* possess substantial quantities of polyphenolic derivatives, including flavonoids, which are regarded as possible bioactive chemicals with antioxidant capabilities. Figure 7 illustrates a comparison of the FTIR spectra for each plant extract, the combined extract, and the

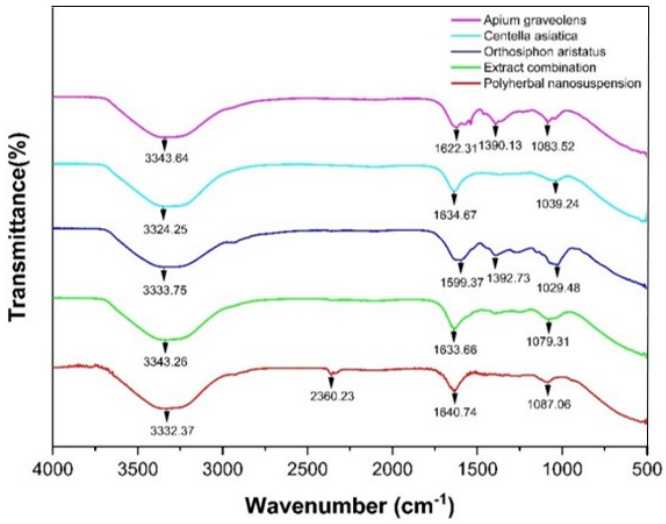

Figure 7. FT-IR Spectroscopy Outcomes

nanopolyherbal formulation.

The FTIR spectra of the individual extracts- A*pium graveolens, Centella asiatica,* and *Orthosiphon aristatus* -along with the extract combination and polyherbal nanosuspension, exhibited notable differences in peak positions and intensities. The variances demonstrate that each sample possesses a unique chemical composition, reflective of the specific phytochemical constituents characteristic of each plant species. The absorption bands observed between 3332 and 3344 cm^{-1} indicate the presence of hydroxyl (−OH) groups, commonly linked to phenolic compounds and alcohols (Udvardi et al., 2017; Albarakaty et al., 2023). These peaks correspond to the O–H stretching vibrations typically observed in plant-derived secondary metabolites. Additionally, peaks identified between 1630 and 1650 cm^{-1} can be attributed to the stretching vibrations of aromatic C=C bonds or carbonyl (C=O) groups. These functional groups are frequently present in triterpenoids and flavonoids, thereby enhancing the phytochemical complexity of the samples (Nomi et al., 2024). The variations in peak positions across samples may indicate molecular interactions or structural changes, particularly in the combined extract and nanosuspension formulations. A notable region is detected around 1390-1392 cm^{-1}, signifying bending vibrations associated with methyl ($-CH_3$) groups or phenolic compounds (Sugunabai et al., 2015). Peaks detected below 1100 cm^{-1} signify C−O stretching vibrations, typically linked to alcohol, ester, or ether functionalities. These peaks validate the presence of numerous chemical functional groups linked to antioxidant or therapeutic properties (Rohman and Ariani, 2013). The FTIR spectra of the extract combination and polyherbal nanosuspension exhibit notable peak shifts or merged absorption bands relative to the individual extracts. This spectral overlap signifies the efficient integration and interaction of numerous phytochemicals, resulting in a complex

Table 12. Stability of Nanopolyherbal Particles at Room Temperature

Parameters	Day-1	Day-15	Day-30	Day-60
color change	greenish clear	greenish clear	greenish clear	greenish clear
Sediment	yes	yes	yes	yes
Particle Size (nm)	220 ± 11.57	221.66±1.41	221.93±0.25	222.60±0.57
Polydispersity Index	0.59±0.06	0.59±0.05	0.61±0.02	0.61±0.05
Zeta Potential (mV)	-28.27±0.37	-28.86±0.55	-27.91±0.15	-27.63±0.54

assortment of bioactive molecules (Pasieczna-Patkowska et al., 2025). Such shifts may also signify molecular compatibility or chemical interaction among the constituent substances. The polyherbal nanosuspension spectrum exhibits an additional absorption peak at 2360.23 cm^{-1}, absent in both the individual extracts and the amalgamation of crude extracts. This unique peak is frequently associated with isocyanate (−N=C=O) or CO_2 stretching vibrations, potentially arising from chemical modifications during nanosuspension preparation or from enhanced molecular interactions at the nanoscale (Chaudhari et al., 2020).

3.6 Antioxidant Activity Assays

3.6.1 DPPH Method

The DPPH method is one of the most commonly used approaches for evaluating the antioxidant activity of a sample, primarily due to its simplicity and cost-effectiveness. In this method, antioxidant compounds neutralize free radicals by donating hydrogen atoms to DPPH molecules, leading to a measurable color change from purple to yellow. The extent of this color shift reflects the compound's ability to reduce DPPH, thereby indicating its antioxidant potential (Mohammed et al., 2016). Figures 8 and 9 display the results of antioxidant testing, specifically the percentage of inhibition and IC_{50} values, for both the extracts and the nano polyherbal formulation. In assessing antioxidant activity, the maximum absorption wavelength (λ max) of DPPH identified in this study was 517 nm, which aligns well with the established range of 515 to 520 nm reported by Mohammed et al. (2016). This wavelength was subsequently used to determine the appropriate incubation period and to analyze both the reference solution and the extracts. Previous research indicates that a 30-minute incubation period is optimal for DPPH analysis; therefore, our test solutions were incubated for 30 minutes under dark conditions. The use of a dark environment is critical to prevent the generation of free radicals other than DPPH, which could interfere with the results (Rosidi, 2020).

As the concentration of the sample solution increases, the measured absorbance value correspondingly decreases. This trend occurs because a higher number of antioxidant molecules are present to neutralize the DPPH radicals (Baliyan et al., 2022). The reduction in absorbance is therefore used to quantify the capacity of antioxidant compounds to scavenge DPPH radicals. By applying linear regression analysis, the relationship between concentration and inhibition can be characterized, with the IC_{50} value serving as an indicator of antioxidant potency-a lower IC_{50} reflects stronger antioxidant activity. An antioxidant's effectiveness is generally indicated by a lower IC_{50} value. To calculate this value, we use a linear regression model that plots sample concentration on the x-axis against percentage inhibition on the y-axis. The IC_{50} value is a common and reliable measure for assessing a sample's antioxidant capacity (Itam et al., 2021). Specifically, we determine the IC_{50} by inputting the percentage inhibition into the regression equation as the dependent variable. A smaller IC_{50} corresponds to stronger antioxidant activity, whereas a larger value suggests weaker activity (Rivero-Cruz et al., 2020).

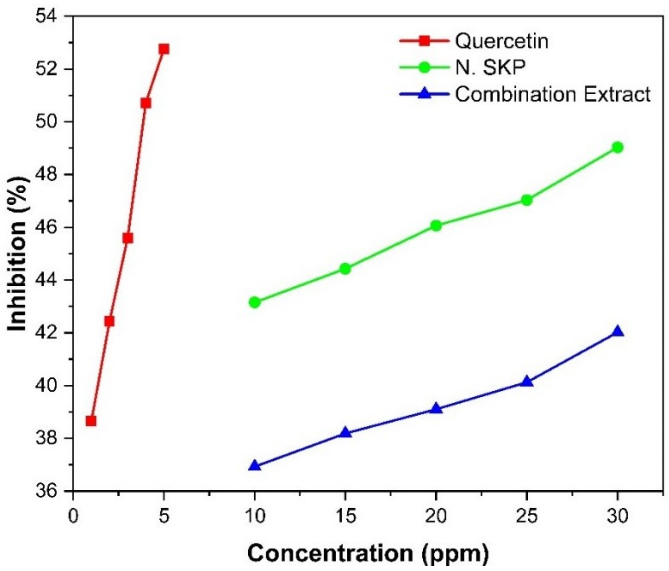

Figure 8. DPPH Radical Scavenging Assay of Standard Quercetin, Combination of Polyherbal and Nanoparticle Polyherbal

The correlation coefficients (R values) for each regression equation were consistently reported at 0.99, indicating a very strong relationship between percentage inhibition and extract concentration. This high value suggests that the concentration of the chemical accounted for 99% of the observed inhibition, with other factors contributing only marginally. In this study, quercetin a flavonoid well recognized for its diverse biological activities and potent free radical scavenging properties served as the standard reference in the antioxidant activity assays. Antiox-

idant activity is categorized by IC_{50} values: IC_{50} <50 μg/mL denotes extreme activity; 50 μg/mL <IC_{50} <100 μg/mL indicates strong activity; 100 μg/mL <IC_{50} <150 μg/mL reflects moderate activity; 150 μg/mL <IC_{50} <200 μg/mL signifies weak activity; and IC_{50} >200 μg/mL represents fragile activity.

The assessment of antioxidant activity using the DPPH method demonstrated that the nanopolymeric formulation containing extracts of celery, cat's whisker, and gotu kola (Nano polyherbals) showed enhanced antioxidant potency, with an IC_{50} value of 41.78 ± 3.064 μg/mL. Notably, this IC_{50} value was lower than that of the extract combination without nanotechnology, which recorded an IC_{50} of 44.93 ± 2.989 μg/mL, indicating improved efficacy in the nano-formulated preparation

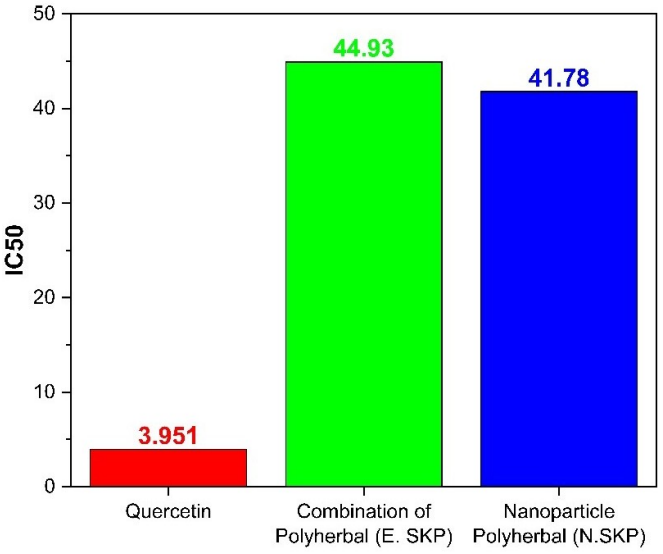

Figure 9. Antioxidant Activity (IC_{50}) by DPPH Radical Scavenging Assay

The findings indicate that nanotechnology-based formulations improve antioxidant effectiveness compared to traditional extracts. This observation is consistent with numerous studies demonstrating that nanotechnology can enhance the antioxidant properties of compounds (Kumar et al., 2020; Pradana et al., 2023). The enhanced antioxidant activity observed in the Nano polyherbals formulations can be attributed to the application of nanopolymeric technology, which improves the preparation's stability and bioavailability, thereby facilitating more efficient delivery of active compounds to target tissues. Moreover, this nanotechnology offers protection to the active compounds against degradation caused by environmental factors such as oxidation, light exposure, or extreme pH conditions, helping to preserve or potentially augment their antioxidant capacity (Aluani et al., 2017).

3.6.2 ABTS Method

The ABTS assay evaluates antioxidant activity by measuring the ability of antioxidants to quench the ABTS cation radical, resulting in decolorization. ABTS is a nitrogen-centered radical characterized by its blue-green color, which becomes colorless upon reduction by antioxidant compounds. (Mareček et al., 2017). The ABTS assay is highly light-sensitive, requiring that tests be performed under dark conditions. The loss of color is indicated by a decrease in absorbance at the assay's maximum wavelength. A calibration curve was generated by plotting the percentage of Trolox decolorization against concentration, ranging from 0 to 250 ppm. The resulting regression equation, y = 0.3511x - 0.2384, with an R^2 value of 0.9991, demonstrates a strong linear relationship. Figures 10 and 11 present the antioxidant activity results, showing the percentage inhibition and IC_{50} values for both the extract combination and the nano polyherbal formulation. For centuries, plants have been recognized as natural reservoirs of bioactive compounds that provide a range of health benefits, including antioxidant effects (Mendonça et al., 2022). The antioxidant qualities of plants are crucial in combating cellular damage induced by free radicals, which can lead to the onset of numerous degenerative diseases and accelerate the aging process (Kasote et al., 2015). Amid increasing concerns over the harmful effects of synthetic chemicals, there is a rising emphasis on plant-based therapies as alternatives to support health and prevent the onset of disease. Today, herbal remedies derived from plants are integral to medical practices in many cultures worldwide. This shift reflects a broader transformation in medicine, highlighting the value of natural resources, with plants recognized as a key source for identifying bioactive compounds for pharmaceutical and preventive applications. Given their wide-ranging therapeutic potentials, plants are increasingly regarded as a sustainable foundation for developing safer and more environmentally friendly treatments (Chaachouay and Zidane, 2024). Antioxidants are molecules that mitigate oxidative damage in biological systems by donating electrons to free radicals, thereby neutralizing their harmful effects (Baliyan et al., 2022). Free radicals are primarily associated with oxidative stress and are produced through the interaction of oxygen with various molecules. Once generated, these reactive species can damage critical biological components such as DNA, proteins, and cell membranes. Antioxidants can neutralize free radicals by reacting with them, thereby preventing potential harm. Plants synthesize a wide range of secondary metabolites, many of which function as antioxidants (Garg et al., 2019).

Antioxidants play a crucial role in protecting cells from damage induced by free radicals, including reactive oxygen species (ROS) (Yan et al., 2023). Numerous chemicals included in herbal plants, such as phenolics, flavonoids, terpenoids, and alkaloids, have demonstrated efficacy as antioxidants, capable of scavenging free radicals (Lourenço et al., 2019). Furthermore, plants possess intrinsic mechanisms to prevent the generation of reactive oxygen species (ROS), including the production of antioxidant compounds that neutralize or deactivate ROS through both chemical and physical processes (Muchtaridi et al., 2024). Flavonoids are widely recognized as powerful antioxidants that neutralize free radicals, chelate metal ions, inhibit en-

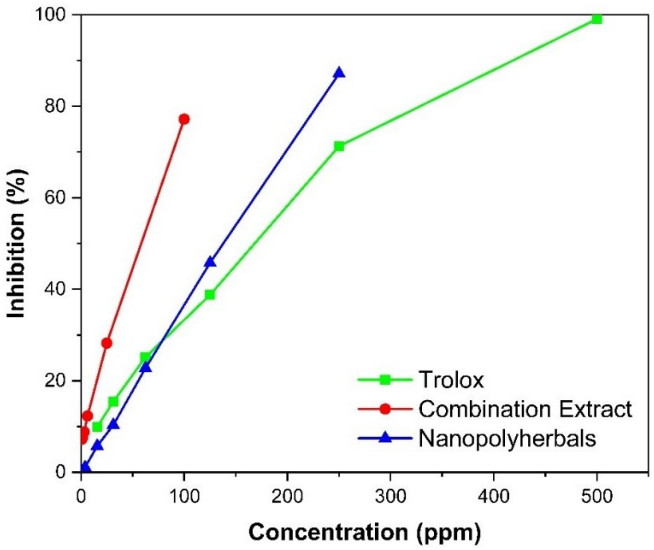

Figure 10. ABTS Radical Scavenging Assay of Standard Trolox, Combination of Polyherbal and Nanoparticle Polyherbal

zymes involved in free radical generation, and boost the body's own antioxidant defenses. Their ability to directly scavenge reactive oxygen species makes flavonoids particularly effective in reducing oxidative damage. Other compounds, such as alkaloids and terpenoids, also contribute to antioxidant activity, thereby strengthening the body's protection against oxidative stress (Hassanpour and Doroudi, 2023; Zahra et al., 2024).

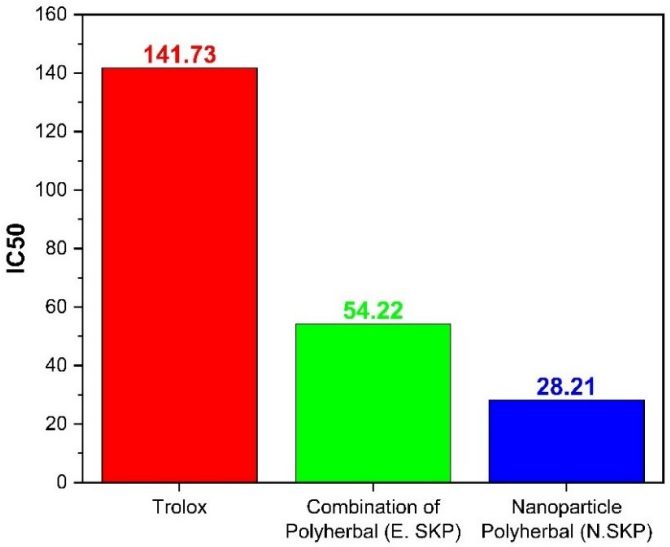

Figure 11. Antioxidant Activity (IC_{50}) by ABTS Radical Scavenging Assay

This study found that the IC_{50} value of the nanopoliherbals formulation was 28.21 μg/mL, indicating a stronger ABTS radical scavenging activity compared to the combined extract. This outcome aligns with the research of Zahra et al. (2024) who indicated that the augmented antioxidant activity in crosslinked nanoparticles is attributable to their reduced particle size, which enhances surface area and facilitates increased absorption of flavonoid chemicals. Furthermore, the ABTS assay revealed stronger antioxidant activity in the nanopoliherbals formulation compared to the DPPH method. This corresponds with the findings of de Silva et al. (2023), which demonstrated that the ABTS assay on alginate nanoparticles of *Coccinia grandis* L. exhibited superior antioxidant activity relative to DPPH. This difference could be attributed to the greater sensitivity of the ABTS assay, which detects antioxidant activity through multiple mechanisms, such as electron transfer and hydrogen atom donation. Additionally, the ABTS method shows a lower coefficient of variation compared to the DPPH assay, indicating more consistent and reliable results (Rumpf et al., 2023).

4. CONCLUSIONS

The study demonstrated that nanosuspensions enhance the antioxidant potency of bioactive compounds derived from *Apium graveolens, Centella asiatica*, and *Orthosiphon stamineus*. The nanosuspension formulated with chitosan, Tween 80, and Na-TPP exhibited a particle size of 220 ± 11.57 nm, a polydispersity index (PDI) of 0.59 ± 0.06, and a zeta potential of –28.27 ± 0.37 mV, indicating improved bioavailability and absorption efficiency. Results from the DPPH and ABTS assays indicated that the nanosuspension exhibited greater antioxidant activity than the combined plant extracts. The lower IC_{50} values observed in both tests highlight the nanosuspension's enhanced capacity to neutralize free radicals. These findings suggest that nanotechnology has the potential to improve the antioxidant properties of bioactive compounds in medicinal plants, thereby providing enhanced health and therapeutic benefits.

5. ACKNOWLEDGMENT

This research received funding by the Directorate of Research, Technology, and Community Service inside of the Ministry of Education, Culture, Research, and Technology in Indonesia, under Grant numbers Nomor: 126/C3/DT.05.00/PL/2025 and 0498.12/LL5-INT/AL.04/2025.

REFERENCES

Abbasnezhad, M., V. Shahabi Raberi, M. Esmati, H. Bodagh, R. Ghasemi, M. Ghazal, and A. Matinpour (2022). The Functionality of Apigenin as a Novel Cardioprotective Nutraceutical with Emphasize on Regulating Cardiac Micro RNAs. *Galen Medical Journal*, **11**(e2535); e2535

Ahmadi Tehrani, A., M. M. Omranpoor, A. Vatanara, M. Seyedabadi, and V. Ramezani (2019). Formation of Nanosuspensions in Bottom-Up Approach: Theories and Optimization. *DARU, Journal of Pharmaceutical Sciences*, **27**(1); 451–473

Akram, W. and N. Garud (2021). Design Expert As a Statistical Tool for Optimization of 5-ASA-Loaded Biopolymer-based

Nanoparticles Using Box Behnken Factorial Design. *Future Journal of Pharmaceutical Sciences*, **7**(1); 146

Albarakaty, F. M., M. I. Alzaban, N. K. Alharbi, F. S. Bagrwan, A. R. M. A. El-Aziz, and M. A. Mahmoud (2023). Zinc Oxide Nanoparticles, Biosynthesis, Characterization and Their Potent Photocatalytic Degradation, and Antioxidant Activities. *Journal of King Saud University – Science*, **35**; 793–797

Aldeeb, M. M. E., G. Wilar, C. Suhandi, A. F. A. Mohammed, S. A. Mahmoud, K. M. Elamin, and N. Wathoni (2025). Emerging Trends in the Application of Nanosuspension-Based Biomaterials for Anticancer Drug Delivery. *International Journal of Nanomedicine*, **20**; 8587–8607

Aluani, D., V. Tzankova, M. Kondeva-Burdina, Y. Yordanov, E. Nikolova, F. Odzhakov, A. Apostolov, T. Markova, and K. Yoncheva (2017). Evaluation of Biocompatibility and Antioxidant Efficiency of Chitosan-Alginate Nanoparticles Loaded with Quercetin. *International Journal of Biological Macromolecules*, **103**; 771–782

Arifin, M. F., Y. Noviani, S. Nafisa, and A. Sheilabel (2022). Preparation, Characterization, and Optimization of Ionic Gelated Nanoparticles Dried Extract of Temulawak Rhizome (Curcuma Xanthorrhiza R.) Using a Factorial Design 2^2. *Jurnal Ilmu Kefarmasian Indonesia*, **20**(2); 272

Astuti, F., Mustofa, A. B. Setianto, and Akrom (2025). Nanotechnology-Based Nanopolymeric Polyherbal Formulation for Enhanced Antioxidant and Anti-Glycation Activity. *Science and Technology Indonesia*, **10**(3); 972–981

Awlqadr, F. H., K. R. Majeed, A. B. Altemimi, A. M. Hassan, S. A. Qadir, M. N. Saeed, A. M. Faraj, T. H. Salih, A. J. A. Al-Manhel, M. A. A. Najm, E. Tsakali, J. F. M. Van Impe, A. A. A. El-Maksoud, and T. G. Abedelmaksoud (2025). Nanotechnology-Based Herbal Medicine: Preparation, Synthesis, and Applications in Food and Medicine. *Journal of Agriculture and Food Research*, **19**

Baliyan, S., R. Mukherjee, A. Priyadarshini, A. Vibhuti, A. Gupta, R. P. Pandey, and C. M. Chang (2022). Determination of Antioxidants by DPPH Radical Scavenging Activity and Quantitative Phytochemical Analysis of *Ficus religiosa*. *Molecules*, **27**(4)

Chaachouay, N. and L. Zidane (2024). Plant-Derived Natural Products: A Source for Drug Discovery and Development. *Drugs and Drug Candidates*, **3**(1); 184–207

Chaudhari, A. K., S. D. Vipin Kumar Singh, Deepika, B. K. Singh, and N. K. Dubey (2020). Antimicrobial, Aflatoxin B1 Inhibitory and Lipid Oxidation Suppressing Potential of Anethole-Based Chitosan Nanoemulsion as Novel Preservative for Protection of Stored Maize. *Food and Bioprocess Technology*, **13**; 1462–1477

Chavda, V. P., D. A. Vaghela, H. K. Solanki, P. C. Balar, S. Modi, and N. R. Gogoi (2025). Nanosuspensions: A New Era of Targeted Therapeutics. *Journal of Drug Delivery Science and Technology*, **105**

Chaves, N., A. Santiago, and J. C. Alías (2020). Quantification of the Antioxidant Activity of Plant Extracts: Analysis of Sensitivity and Hierarchization Based on the Method Used. *Antioxidants*, **9**(1); 76

Chavhan, R. (2025). Nanosuspensions: Enhancing Drug Bioavailability Through Nanonization / Nanosuspensions: Améliorer la Biodisponibilité des Médicaments Par la Nanonisation. *Annales Pharmaceutiques Françaises*, **83**(2); 251–271

Cruz-Casas, D. E., C. N. Aguilar, J. A. Ascacio-Valdés, R. Rodríguez-Herrera, M. L. Chávez-González, and A. C. Flores-Gallegos (2023). Bioactive Protein Hydrolysates Obtained From Amaranth by Fermentation With Lactic Acid Bacteria and Bacillus Species. *Heliyon*, **9**(2); e13491

Danaei, M., M. Dehghankhold, S. Ataei, F. Hasanzadeh Davarani, R. Javanmard, A. Dokhani, S. Khorasani, and M. R. Mozafari (2018). Impact of Particle Size and Polydispersity Index on the Clinical Applications of Lipidic Nanocarrier Systems. *Pharmaceutics*, **10**(2); 57

de Silva, W. N. D., A. P. Attanayake, L. D. A. M. Arawwawala, D. N. Karunaratne, and G. K. Pamunuwa (2023). In Vitro Antioxidant Activity of Alginate Nanoparticles Encapsulating the Aqueous Extract of Coccinia Grandis L. *Turkish Journal of Chemistry*, **47**(4); 715–725

Dubale, S., D. Kebebe, A. Zeynudin, N. Abdissa, and S. Suleman (2023). Phytochemical Screening and Antimicrobial Activity Evaluation of Selected Medicinal Plants in Ethiopia. *Journal of Experimental Pharmacology*, **15**; 51–62

Emad, A. M., D. M. Rasheed, R. F. El-kased, and D. M. Elkersh (2022). *Apium Graveolens* L. (Apiaceae) Aerial Parts: Phytochemical Analysis and Bioactivity. *Molecules*, **27**; 698

Fan, W., W. Yan, Z. Xu, and H. Ni (2012). Formation Mechanism of Monodisperse, Low Molecular Weight Chitosan Nanoparticles by Ionic Gelation Technique. *Colloids and Surfaces B: Biointerfaces*, **90**; 21–27

Garg, P., R. Garg, and C. P. Garg (2019). Phytochemical Screening and Quantitative Estimation of Total Flavonoids of Ocimum Sanctum in Different Solvent Extract. *The Pharma Innovation Journal*, **8**(2); 16–21

Godge, G. R., M. A. Garje, A. B. Dode, and K. N. Tarkase (2020). Nanosuspension Technology for Delivery of Poorly Soluble Drugs and Its Applications: A Review. *International Journal of Pharmaceutical Sciences and Nanotechnology (IJPSN)*, **13**(4); 4965–4978

Hafiz, Z. Z., M. Amin, R. M. Johari James, L. K. Teh, M. Z. Salleh, and M. I. Adenan (2020). Inhibitory Effects of Raw-Extract *Centella asiatica* (RECA) on Acetylcholinesterase, Inflammations, and Oxidative Stress Activities via In Vitro and In Vivo. *Molecules*, **25**(4); 892

Han Jie, L., I. Jantan, S. D. Yusoff, J. Jalil, and K. Husain (2021). Sinensetin: An Insight on Its Pharmacological Activities, Mechanisms of Action and Toxicity. *Frontiers in Pharmacology*, **11**; 553404

Hassanpour, S. H. and A. Doroudi (2023). Review of the Antioxidant Potential of Flavonoids as a Subgroup of Polyphenols and Partial Substitute for Synthetic Antioxidants. *Avicenna Journal of Phytomedicine*, **13**(4); 354–376

Heinz, H., C. Pramanik, O. Heinz, Y. Ding, R. K. Mishra,

D. Marchon, R. J. Flatt, I. Estrela-Lopis, J. Llop, S. Moya, and R. F. Ziolo (2017). Nanoparticle Decoration With Surfactants: Molecular Interactions, Assembly, and Applications. *Surface Science Reports*, **72**(1); 1–58

Hizar, S. A. K., N. R. Putra, R. Kobun, S. F. M. Amin, J. Roslan, M. E. Ronie, M. A. A. Zaini, H. Mamat, and A. H. A. Aziz (2024). Subcritical Water Extraction on Phenolic, Flavonoid and Antioxidant Activity From *Orthosiphon stamineus* Leaves: Experimental and Optimization. *Journal of Engineering Research*; 1–8

Ho, S. K., C. P. Tan, Y. Y. Thoo, F. Abas, and C. W. Ho (2014). Ultrasound-Assisted Extraction of Antioxidants in Misai Kucing (*Orthosiphon stamineus*). *Molecules*, **19**(8); 12640–12659

Huang, L., X.-H. Huang, X. Yang, J.-Q. Hu, Y.-Z. Zhu, P.-Y. Yan, and Y. Xie (2024). Novel Nano-Drug Delivery System for Natural Products and Their Application. *Pharmacological Research*, **201**; 107132

Itam, A., M. S. Wati, V. Agustin, N. Sabri, R. A. Jumanah, and M. Efdi (2021). Comparative Study of Phytochemical, Antioxidant, and Cytotoxic Activities and Phenolic Content of *Syzygium aqueum* (Burm. f. Alston f.) Extracts Growing in West Sumatera Indonesia. *Scientific World Journal*, **2021**; 1–9

Jacob, S., F. S. Kather, S. H. S. Boddu, M. Attimarad, and A. B. Nair (2025). Nanosuspension Innovations: Expanding Horizons in Drug Delivery Techniques. *Pharmaceutics*, **17**(1); 1–61

Jahan, N., F. Kousar, K. U. Rahman, S. I. Touqeer, and N. Abbas (2023). Development of Nanosuspension of *Artemisia absinthium* Extract as Novel Drug Delivery System to Enhance Its Bioavailability and Hepatoprotective Potential. *Journal of Functional Biomaterials*, **14**(8); 1–19

Jankovic, A. and F. G. G. Chaudhary (2021). Designing the Design of Experiments (DOE)–An Investigation on the Influence of Different Factorial Designs on the Characterization of Complex Systems. *Energy and Buildings*, **250**; 111307

Kandasamy, A., K. Aruchamy, P. Rangasamy, and D. Varadhaiyan (2023). Phytochemical Analysis and Antioxidant Activity of *Centella asiatica* Extracts: An Experimental and Theoretical Investigation of Flavonoids. *Not Provided*, **12**(20); 3547

Kasote, D. M., S. S. Katyare, M. V. Hegde, and H. Bae (2015). Significance of Antioxidant Potential of Plants and Its Relevance to Therapeutic Applications. *International Journal of Biological Sciences*, **11**(8); 982–991

Kaur, H., S. Ghosh, P. Kumar, B. Basu, and K. Nagpal (2021). Ellagic Acid-Loaded, Tween 80-Coated, Chitosan Nanoparticles as a Promising Therapeutic Approach Against Breast Cancer: In-Vitro and In-Vivo Study. *Life Sciences*, **284**; 119930

Kazi, M., A. Alhajri, S. M. Alshehri, E. M. Elzayat, O. T. Al Meanazel, F. Shakeel, O. Noman, M. A. Altamimi, and F. K. Alanazi (2020). Enhancing Oral Bioavailability of Apigenin Using a Bioactive Self-Nanoemulsifying Drug Delivery System (Bio-SNEDDS): In Vitro, In Vivo and Stability Evaluations. *Pharmaceutics*, **12**(8); 749

Kheradkar, V. A. and J. A. S. M. (2023). Nanosuspension: A Novel Technology for Drug Delivery. *Sian Journal of Research in Pharmaceutical Sciences*, **13**(2); 106

Kumar, H., K. Bhardwaj, E. Nepovimova, K. Kuča, D. S. Dhanjal, S. Bhardwaj, S. K. Bhatia, R. Verma, and D. Kumar (2020). Antioxidant Functionalized Nanoparticles: A Combat Against Oxidative Stress. *Nanomaterials*, **10**(7); 1369

Kumar, S. and A. K. Pandey (2013). Chemistry and Biological Activities of Flavonoids: An Overview. *The Scientific World Journal*, **2013**; 1–16

Li, M., M. Azad, R. Davé, and E. Bilgili (2016). Nanomilling of Drugs for Bioavailability Enhancement: A Holistic Formulation-Process Perspective. *Pharmaceutics*, **8**(2); 1–20

Liu, J., L. Tu, M. Cheng, J. Feng, and Y. Jin (2020). Mechanisms for Oral Absorption Enhancement of Drugs by Nanocrystals. *Journal of Drug Delivery Science and Technology*, **56**; 101533

Liu, Y., Y. Liang, J. Yuhong, P. Xin, J. L. Han, R. Zhu, M. Zhang, W. Chen, Y. Ma, Y. Du, and X. Yu (2024). Advances in Nanotechnology for Enhancing the Solubility and Bioavailability of Poorly Soluble Drugs. *Drug Design, Development and Therapy*, **18**; 1469–1495

López-León, T., E. L. S. Carvalho, B. Seijo, J. L. Ortega-Vinuesa, and D. Bastos-González (2005). Physicochemical Characterization of Chitosan Nanoparticles: Electrokinetic and Stability Behavior. *Journal of Colloid and Interface Science*, **283**(3); 344–351

Lourenço, S. C., M. Moldão-Martins, and V. D. Alves (2019). Antioxidants of Natural Plant Origins: From Sources to Food Industry Applications. *Molecules*, **24**(22); 4132

Lukman, L., N. Rosita, and R. Widyowati (2024). Assessment of Antioxidant Activity, Total Phenolic and Flavonoid Contents of *Albizia saponaria* L. Bark Extract. *Science and Technology Indonesia*, **9**(2); 494–501

Maity, S., P. Mukhopadhyay, P. P. Kundu, and A. S. Chakraborti (2017). Alginate Coated Chitosan Core-Shell Nanoparticles for Efficient Oral Delivery of Naringenin in Diabetic Animals—An In Vitro and In Vivo Approach. *Carbohydrate Polymers*, **170**; 124–134

Mareček, V., A. M. A, D. Hampel, P. Čejka, J. Neuwirthová, A. Malachová, and R. Cerkal (2017). ABTS and DPPH Methods as a Tool for Studying Antioxidant Capacity of Spring Barley and Malt. *Journal of Cereal Science*, **73**; 40–45

Mendonça, J. d. S., R. d. C. A. Guimarães, V. A. Zorgetto-Pinheiro, C. D. P. Fernandes, G. Marcelino, D. Bogo, K. d. C. Freitas, P. A. Hiane, E. S. d. P. Melo, M. L. B. Vilela, and V. A. Do Nascimento (2022). Natural Antioxidant Evaluation: A Review of Detection Methods. *Molecules*, **27**(11); 3401

Mohammed, N. K., M. Yazid, A. Manap, C. P. Tan, B. J. Muhialdin, A. M. Alhelli, A. Shobirin, and M. Hussin (2016). The Effects of Different Extraction Methods on Antioxidant Properties, Chemical Composition, and Thermal Behav-

ior of Black Seed (Nigella Sativa L.) Oil. *Evidence-Based Complementary and Alternative Medicine*, **2016**; 6273817

Mohamud Dirie, L., T. Yurdakul, S. Isik, and S. Tarbiat (2025). Exploring the Neuroprotective Properties of Celery (*Apium graveolens* Linn) Extract Against Amyloid-Beta Toxicity and Enzymes Associated with Alzheimer's Disease. *Molecules*, **30**(10); 2187

Muchtaridi, M. Darmawan, M. Elizabeth, D. Nurzanah, P. Margaretha, A. A. Elaine, Neli, N. Puspitadewi, L. U. Setyawati, and N. K. K. Ikram (2023). Interactions of *Orthosiphon stamineus* Compounds Against Cox-2 as an Antiinflammatory Using in Silico Methods and Toxicity Prediction. *International Journal of Applied Pharmaceutics*, **15**(6); 288–296

Muchtaridi, M., F. Az-Zahra, H. Wongso, L. U. Setyawati, D. Novitasari, and E. H. K. Ikram (2024). Molecular Mechanism of Natural Food Antioxidants to Regulate ROS in Treating Cancer: A Review. *Antioxidants*, **13**(2); 1–18

Nafisa, S., S. U. Noor, A. Azkannufuus, and Y. Noviani (2023). Cosmos Caudatus Kunth. Leaf Extract Herbal Nanosuspension Formulations, Characterization, and Cytotoxicity Approach Against MCF-7 Breast Cancer Cells. *Jurnal Ilmu Kefarmasian Indonesia*, **21**(2); 286–294

Narukulla, S., S. Bogadi, V. Tallapaneni, B. K. R. Sanapalli, S. Sanju, A. A. Khan, A. Malik, H. R. Barai, T. K. Mondal, V. V. S. R. Karri, A. Alexiou, S. K. S. S. Pindiprolu, G. Kuppusamy, V. Subramaniyan, M. R. Islam, and M. Papadakis (2024). Comparative Study Between the Full Factorial, Box–Behnken, and Central Composite Designs in the Optimization of Metronidazole Immediate Release Tablet. *Microchemical Journal*, **207**; 111875

Németh, Z., I. Csóka, R. Semnani Jazani, B. Sipos, H. Haspel, G. Kozma, Z. Kónya, and D. G. Dobó (2022). Quality by Design-Driven Zeta Potential Optimisation Study of Liposomes With Charge Imparting Membrane Additives. *Pharmaceutics*, **14**(9); 1798

Nomi, A. G., H. Handayani, R. H. Khuluk, A. H. Karomah, L. Wulansari, N. D. Yuliana, E. Rohaeti, and M. Rafi (2024). Antioxidant Activity and Metabolite Changes in *Centella asiatica* With Different Drying Methods Using FTIR- and Quantitative HPLC-Based Metabolomics. *International Food Research Journal*, **31**(1); 228–238

Pakki, E., R. Tayeb, U. Usmar, I. Ridwan, and L. Muslimin (2020). Effect of Orally Administered Combination of Caulerpa Racemosa and Eleutherine Americana (Aubl) Merr Extracts on Phagocytic Activity of Macrophage. *Research in Pharmaceutical Sciences*, **15**(4); 401–409

Pasieczna-Patkowska, S., M. Cichy, and J. Flieger (2025). Application of Fourier Transform Infrared (FTIR) Spectroscopy in Characterization of Green Synthesized Nanoparticles. *Molecules*, **30**(3); 684

Patel, V. and Y. Agrawal (2011). Nanosuspension: An Approach To Enhance Solubility of Drugs. *Journal of Advanced Pharmaceutical Technology & Research*, **2**(2); 81–87

Pereira, I., A. Zielińska, N. R. Ferreira, A. M. Silva, and E. B. Souto (2018). Optimization of Linalool-Loaded Solid Lipid Nanoparticles Using Experimental Factorial Design and Long-Term Stability Studies With a New Centrifugal Sedimentation Method. *International Journal of Pharmaceutics*, **549**(1-2); 261–270

Pınar, S. G., A. N. Oktay, A. E. Karaküçük, and N. Çelebi (2023). Formulation Strategies of Nanosuspensions for Various Administration Routes. *Pharmaceutics*, **15**(5); 1520

Pradana, T. B., A. E. Nugroho, and R. Martien (2023). Systematic Review: Nanopartikel Dari Bahan Dalam Obat Tradisional Indonesia. *Majalah Farmaseutik*, **19**(4); 2023

Puspadewi, R., T. Milanda, M. Muhaimin, and A. Y. Chaerunisaa (2025). Nanoparticle-Encapsulated Plant Polyphenols and Flavonoids as an Enhanced Delivery System for Anti-Acne Therapy. *Pharmaceuticals*, **18**(2); 209

Rivero-Cruz, J. F., J. Granados-Pineda, J. Pedraza-Chaverri, J. M. Pérez-Rojas, A. Kumar-Passari, G. Diaz-Ruiz, and B. E. Rivero-Cruz (2020). Phytochemical Constituents, Antioxidant, Cytotoxic, and Antimicrobial Activities of the Ethanolic Extract of Mexican Brown Propolis. *Antioxidants*, **9**(1); 70

Rohman, A. and R. Ariani (2013). Authentication of Nigella Sativa Seed Oil in Binary and Ternary Mixtures With Corn Oil and Soybean Oil Using FTIR Spectroscopy Coupled With Partial Least Square. *The Scientific World Journal*, **2013**; 1–6

Rosidi, A. (2020). The Difference of Curcumin and Antioxidant Activity in Curcuma Xanthorrhiza at Different Regions. *Journal of Advanced Pharmacy Education & Research*, **10**(1); 14–18

Rumpf, J., R. Burger, and M. Schulze (2023). Statistical Evaluation of DPPH, ABTS, FRAP, and Folin-Ciocalteu Assays To Assess the Antioxidant Capacity of Lignins. *International Journal of Biological Macromolecules*, **233**; 123470

S, S., A. Nair, M. P. Prathapan, N. S, and N. Kumar (2017). Phytochemical Analysis of *Centella asiatica* L. Leaf Extracts. *International Journal of Advanced Research*, **5**(6); 1828–1832

Scolari, I. R., P. L. Páez, M. E. Sánchez-Borzone, and G. E. Granero (2019). Promising Chitosan-Coated Alginate-Tween 80 Nanoparticles as Rifampicin Coadministered Ascorbic Acid Delivery Carrier Against Mycobacterium Tuberculosis. *AAPS PharmSciTech*, **20**(7); 270

Singh, M. K., D. Pooja, H. G. Ravuri, A. Gunukula, H. Kulhari, and R. Sistla (2018). Fabrication of Surfactant-Stabilized Nanosuspension of Naringenin To Surpass Its Poor Physiochemical Properties and Low Oral Bioavailability. *Phytomedicine*, **40**; 48–54

Sivakumar, C. and K. Jeganathan (2018). Phytochemical Profiling of Cat Whisker's (*Orthosiphon stamineus*) Tea Leaves Extract. *Journal of Pharmacognosy and Phytochemistry*, **7**(6); 1396–1402

Sugunabai, J., M. Jeyaraj, and T. Karpagam (2015). Analysis of Functional Compounds and Antioxidant Activity of *Centella asiatica*. *World Journal of Pharmacy and Pharmaceutical Sciences*, **4**(8); 1982–1993

Sulastri, E., M. S. Zubair, N. I. Anas, S. Abidin, R. Hardani,

R. Yulianti, and Aliyah (2018). Total Phenolic, Total Flavonoid, Quercetin Content and Antioxidant Activity of Standardized Extract of Moringa Oleifera Leaf From Regions With Different Elevation. *Pharmacognosy Journal*, **10**(6); S104–S108

Sultana, S., I. L. Lawag, L. Y. Lim, K. J. Foster, and C. Locher (2024). A Critical Exploration of the Total Flavonoid Content Assay for Honey. *Methods and Protocols*, **7**(6); 1–17

Susanti, N., A. Mustika, J. Khotib, R. Muti'ah, and M. Rochmanti (2023). Phytochemical, Metabolite Compound, and Antioxidant Activity of Clinacanthus Nutans Leaf Extract From Indonesia. *Science and Technology Indonesia*, **8**(1); 38–44

Syukur, M., M. S. Prahasiwi, Nurkhasanah, S. Yuliani, Y. Purwaningsih, and E. Indriyanti (2023). Profiling of Active Compounds of Extract Ethanol, n-Hexane, Ethyl Acetate and Fraction Ethanol of Star Anise (Illicium Verum Hook. f.) and Determination of Total Flavonoids, Total Phenolics and Their Potential as Antioxidants. *Science and Technology Indonesia*, **8**(2); 219–226

Udvardi, B., I. J. Kovács, T. Fancsik, P. Kónya, M. Bátori, F. Stercel, G. Falus, and Z. Szalai (2017). Effects of Particle Size on the Attenuated Total Reflection Spectrum of Minerals. *Applied Spectroscopy*, **71**(6); 1157–1168

Wang, H., Y. Chen, L. Wang, Q. Liu, S. Yang, and C. Wang (2023). Advancing Herbal Medicine: Enhancing Product Quality and Safety Through Robust Quality Control Practices. *Frontiers in Pharmacology*, **14**; 1–16

Wei, Y., Y. Zhang, B. Zhan, Y. Wang, J. Cheng, H. Yu, M. Lv, Y. Zhang, Y. Zhai, Y. Guan, and H. Feng (2025). Asiaticoside Alleviated NAFLD by Activating Nrf2 and Inhibiting the NF-k. *Phytomedicine*, **136**; 156317

Weissman, S. A. and N. G. Anderson (2015). Design of Experiments (DoE) and Process Optimization: A Review of Recent Publications. *Organic Process Research & Development*, **19**(11); 1605–1633

Yan, Q., S. Liu, Y. Sun, C. Chen, S. Yang, M. Lin, J. Long, J. Yao, Y. Lin, F. Yi, L. Meng, Y. Tan, Q. Ai, N. Chen, and Y. Yang (2023). Targeting Oxidative Stress as a Preventive and Therapeutic Approach for Cardiovascular Disease. *Journal of Translational Medicine*, **21**(1); 1–35

Zahra, M., H. Abrahamse, and B. P. George (2024). Flavonoids: Antioxidant Powerhouses and Their Role in Nanomedicine. *Antioxidants*, **13**(8); 922

Zhou, F., T. Peterson, Z. Fan, and S. Wang (2023). The Commonly Used Stabilizers for Phytochemical-Based Nanoparticles: Stabilization Effects, Mechanisms, and Applications. *Nutrients*, **15**(18); 3881

Zhuo, Y., Y. G. Zhao, and Y. Zhang (2024). Enhancing Drug Solubility, Bioavailability, and Targeted Therapeutic Applications Through Magnetic Nanoparticles. *Molecules*, **29**(20); 1–35

